Evaluation of Open Cell Foam Heat Transfer Enhancement for Liquid Rocket Engines

J. N. Chung, Landon Tully, Jung Hwan Kim
Department of Mechanical and Aerospace Engineering
University of Florida
Gainesville, Florida

Gregg W. Jones
NASA Marshall Space Flight Center
Huntsville, Alabama

William Watkins
Pratt & Whitney Rocketdyne
West Palm Beach, Florida

ABSTRACT

As NASA pursues the exploration mission, advanced propulsion for the next generation of spacecraft will be needed. These new propulsion systems will require higher performance and increased durability, despite current limitations on materials. A break-through technology is needed in the thrust chamber. In this paper the idea of using a porous metallic foam is examined for its potential cooling enhancement capabilities. The goal is to increase the chamber wall cooling without creating an additional pressure drop penalty.

A feasibility study based on experiments at laboratory-scale conditions was performed and analysis at rocket conditions is underway. In the experiment, heat transfer and pressure drop data were collected using air as the coolant in a copper or nickel foam filled annular channel. The foam-channel performance was evaluated based on comparison with conventional microchannel cooling passages under equal pressure drop conditions. The heat transfer enhancement of the foam channel over the microchannel ranges from 130% to 172%. The enhancement is relatively independent of the pressure drop and increases with decreasing pore size.

A direct numerical simulation model of the foam heat exchange has been built. The model is based on the actual metal foam microstructure of thin ligaments (0.2-0.3 mm in diameter) that form a network of interconnected open-cells. The cell dimension is around 2 mm. The numerical model was built using the FLUENT CFD code. Comparison of the pressure drop results predicted by the current model with those experimental data of Leong and Jin [8] shows favorable comparisons. Pressure drop predictions have been made using hydrogen as a coolant at typical rocket conditions. Conjugate heat transfer analysis using the foam filled channel is planned for the future.

Introduction and Background

Modern rocket engines require actively cooled chamber walls to achieve high performance. Active cooling protects the chamber structure from the extremely hot (+3000 K) combustion gases in addition to preheating the rocket propellants prior to introduction into the combustion chamber. Even with new advances in high-temperature and high conductivity materials, thrust increases for large liquid propellant rocket engines are limited by the cooling capacity of the cooling jacket. Cooling limits have been extended with the use of film cooling, injector biasing, and transpiration cooling. However, these methods are costly to engine performance since they require that some of the fuel pass through the thrust chamber throat without contributing to thrust.

Currently, the vast majority of regeneratively cooled rocket engines use either tube bundles or milled rectangular passages as heat exchangers. This paper presents an alternate cooling methodology that has the potential to double the cooling capacity of the heat exchanger without increase in pressure drop. The alternate method uses cooling passages filled with a high-conductivity porous medium, open-cell foam.

Koh and Colony [1] and Koh and Stevens [2] investigated the enhancement of heat transfer for forced-convection in a channel filled with a high thermal conductivity porous medium. In their theoretical study, Koh and Colony [1] found that for a fixed wall temperature case, the heat transfer rate increased by a factor of three. For a constant heat flux case, the wall temperature and the temperature difference between the wall and the coolant can be drastically reduced. Koh and Stevens (1975) performed experimental work to verify the numerical results of Koh and Colony [1]. Koh and Stevens [2] used a stainless steel cylindrical annulus (1.5" ID and 2.1" OD) with a length of 8 in. to experiment with heat transfer enhancement by a porous filler. The annulus was filled with peen shot (steel particles) having diameters of from 0.08 in. to 0.11 in. Nitrogen gas was the coolant . They found the heat flux increased from 17 to 37 Btu/ft^2s for a constant wall temperature case and the wall temperature dropped from 1450 ^oF to 350 ^oF for the constant heat flux case. Hunt and Tien [3] utilized foam-like material and fibrous media to enhance forced-convection for potential application to electronics cooling. Their results showed that a factor of two to four times enhancement is achievable as compared to laminar slug flow in a duct. Maiorov et al. [4] found empirically that the heat transfer rates in channels with a high-thermal conductivity filler, compared to empty channels, reached a factor of 25-40 enhancement for water and 200-400 for nitrogen gas. Bartlett and Viskanta [5] developed a mathematical model to predict the enhancement by high thermal conductivity porous media in forced-convection duct flows. They concluded that a 5-30 times increase in heat transfer is feasible for most engineering conditions. It is believed that the enhancement is mainly due to the micro turbulent mixing in the pores and super heat transfer through high thermal conductivity porous structure.

Kuzay et al. [6] have reported liquid nitrogen convective heat transfer enhancement with copper matrix inserts in tubes. They proved that the insertion of porous copper mesh into plain tubes enhances the heat transfer by large amounts with a single–phase coolant. However, in boiling, with tubes in which the porous insert is brazed to the tube wall for

the best thermal contact, the heat enhancement is to be on the order of four-fold relative to a plain tube. They conclude that porous matrix inserts offer a significant advantage in cooling, providing a jitter-free operation and a much higher effective heat transfer, at grossly reduced flow rates relative to plain tubes.

More recently, Boomsma et al.[7] used a open-cell aluminum alloy metal foam measuring 40 mm x 40 mm x 2mm as a compact heat exchanger. With liquid water as the working fluid, they found that the heat exchanger generated resistances that are two to three times lower than those of the open channel heat exchanger while requiring the same pumping power.

Porous media heat exchangers have the potential for large increases in cooling capacity of current rocket heat exchangers. The above examples demonstrated large cooling capacity improvements at low Reynolds number conditions. To obtain similar improvements with rocket chamber heat exchangers, porous media must be engineered for conditions found in rocket chamber heat exchangers, i.e., high Reynolds numbers. This paper documents research to demonstrate the feasibility for improved cooling capability of open-cell foam filled heat exchangers for the rocket engine environment.

Objective

The objective of this work is to evaluate effectiveness of open cell foam porous media as applied to rocket engine heat exchangers.

Approach

The approach combines analysis and experiment. A step-wise building-block approach was formulated:

- Heat transfer enhancement was demonstrated in laboratory experiments at low Reynolds numbers, and the Reynolds number range was extended from the literature data base (Re~10,000 to ~40,000). Special attention was paid to accompanying pressure drops.
- An analytical model of open cell foam-filled cooling passages was created. The model was used to model the laboratory experiments and predict heat transfer rates and pressure drops. Comparison of lab experiment results with analytical model results were made to benchmark the analytical model.
- The analytical model was applied to a representative rocket engine condition. A generic rocket engine set of parameters was developed from AIAA Paper 2005-4302, "Supercritical Flows in High Aspect Ratio Cooling Channels" (reference 11). Models of both conventional, un-filled channels and channels filled with open-cell foam are underway.
- With success in the above tasks, design, fabrication and test is planned for a representative heat exchanger segment to be tested at rocket engine operating conditions.

Fabrication and test of rocket hardware involves commitment and expenditure of much larger amounts of funding than analysis and simple laboratory experiments. A success criteria for the laboratory experiment and analysis phase have been developed for the requirements to proceed with representative rocket hardware.

- Large increase in heat transfer: the analysis must predict that large (~>1.5x) increases in heat transfer will be obtained at rocket conditions.
- No increase in pressure drop: the analysis must predict that heat transfer increases are obtainable without increase in pressure drop relative to a conventional, un-filled cooling channel.
- Structural viability: a structural analysis must predict that the foam-filled cooling channel is structurally adequate for the projected operating conditions.
- Fabricability: a demonstration must be done of bonding open cell foam to the channel walls.

The above approach meets the requirements of NASA's Constellation University and Institute Program (CUIP), which seeks to join University research with NASA's needs for designing advanced propulsion systems capable of returning to the moon and eventually to Mars and beyond.

Experiment

The experiment consisted of a test section, inlet region, outlet region, a flow meter, flow valves and a data acquisition system. Fig. 1 shows a schematic of the experiment.

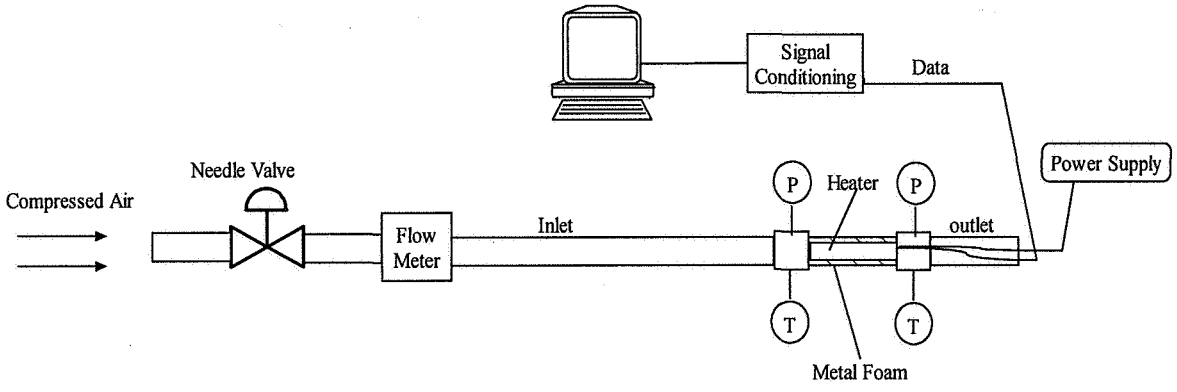

Fig. 1. Schematic of experiment

Compressed air was supplied to the experimental system with a maximum pressure of 200 psi. The needle valve was used to regulate the flow. The flow meter (King Instrument 7700 Series) had a full scale up to 100 cfm (cubic foot per minute) and an accuracy of ±3%.

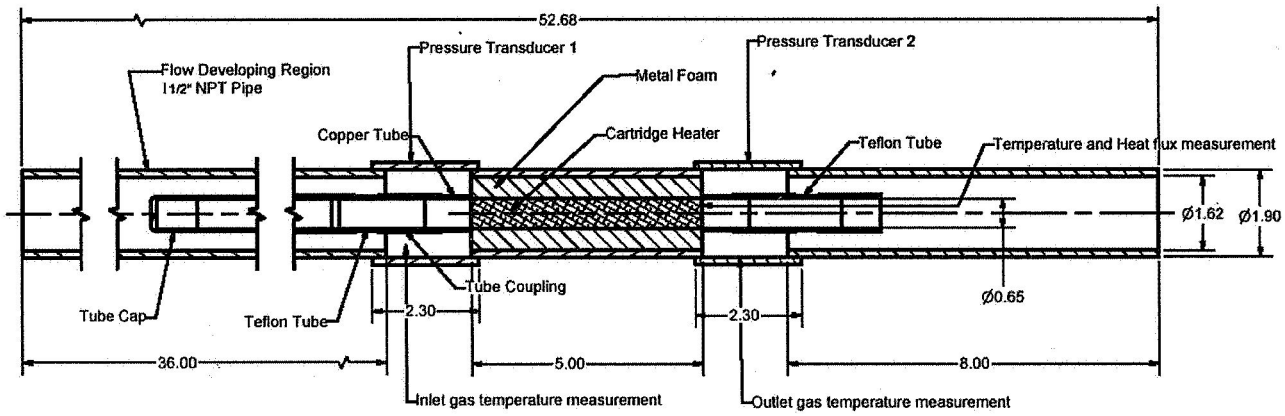

Fig. 2. Schematic of the test section

Two types of test sections were used in the experiment. One was an annulus with copper metal foam insert that was brazed to the inner wall while the other was an open-annulus with the same dimensions. For the metal foam test section, the annular metal foam had a 1.62" OD and a length of 5" that was brazed on the stainless steel pipes of 1.05" OD. The length of the pipes was 7". A 5" long cartridge heater was inserted into a 5" long copper tube, and then the copper tube was wrapped with very thin copper film and firmly inserted into the test section to provide a constant heat flux. To minimize the axial heat transfer, the copper tube was coupled with two Teflon tubes of 2.5" length at both ends. A 25" long copper tube capped with one end was connected to one of the Teflon tube and inserted inside the inlet region. This ensured the air flow to be fully developed before it went into the test section. The inside of the test section was a 5" long aluminum pipe. Fiberglass insulation was placed around the aluminum pipe. Fig. 2 gives the dimensions of the test section and a detailed view of how the system was assembled. The open-channel test section had the same dimensions as the metal foam test section except that no metal foam was on the stainless steel pipe. Therefore, the air flow went through the annulus between the test section and the aluminum pipe. The open-channel test was used as a calibration and as a basis for comparison to the metal foam test.

The copper metal foam was purchased from the Porvair Company. The foam had a layered structure as shown in Figure 3 and the cells had a pentagonal shape. For the foam used the cell size is around 2.5 mm (10 pores per inch or 10 ppi). The ligaments had an average thickness of 300 microns. The porosity was 95%, i.e., the relative density was 5%. Brazing of the metal foam onto the wall was performed by Porvair with metal foil and pressing under elevated temperatures.

The data collected during the experiments were flow rate, pressure and temperature. The flow rate was adjusted by the needle valve and measured by the flow meter; it remained constant in each test. Two flow meters were used in the test. For flow rate larger than 20cfm (cubic foot per minute) a King Instrument 7700 Series with full scale up to 100 cfm and accuracy of 3% was used. An Omega FL4514 flow meter with a full scale accuracy of 2% was used for flow rate from 6.0cfm to 20cfm.

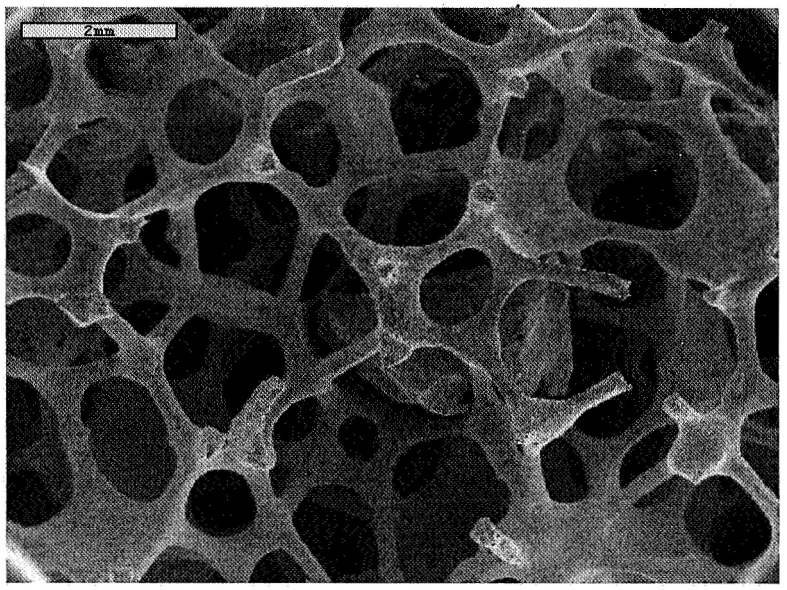

Figure 3. A SEM photograph of the copper foam.

An Omega PX203-200G5V pressure transducer of 0.25% FS accuracy was used to measure the inlet pressure at the inlet region. Accurate measurement of the pressure loss characteristic of metal foam was very important. A differential pressure transducer (Validyne DP1540N1S4A) with changeable diaphragms was used to measure the pressure drop across the test section. Two diaphragms were used in the test (Validyne 3-22 and 3-40); both diaphragms had a 0.25% FS accuracy and could be over pressured up to 200%. The pressure range of Validyne 3-22 was 0-0.20psi and the pressure range of Validyne 3-40 was 0-12.5psi. The pressure transducer was powered by a Validyne DP16A1A demodulator and produced a 0-5V signal. Each time the diaphragm was changed the pressure transducer was recalibrated. Sixteen thermocouples were used at different downstream locations. Five type K thermocouples with fiberglass insulation were used to measure the outside wall temperatures of the test section. Both the air flow inlet and outlet temperatures were measured with 3 type T thermocouples. The inlet and outlet air temperature was then the average of these three temperatures. The average of these two temperatures was used as the bulk temperature of the air flow. The difference of these two temperatures was used in the energy balance to calculate the heat carried by the air flow. Four type T thermocouples were placed at different locations before and after the test section and measurements were used to calculate the axial heat leakage. The outside wall temperature of the test section was also measured and used to calculate the heat loss to the environment. All thermocouples were connected to a 16-channel screw terminal board and then to Measurement Computing PCI-DAS-TC A/D boards. A/D boards were plugged into the PCI slot of a computer. A Labview program was written to control both pressure and the temperature acquisition.

First, the needle valve was opened to the maximum and the cartridge heater was turned on. The compressed air passed through the experiment at the maximum flow rate. Steady-state was considered to be attained when the temperatures indicated by the thermocouples did not vary more than $\pm 0.3^{\circ}C$ within 1 minute. This usually required approximately 1.5-2.0 hours. After reaching steady-state, the needle valve was adjusted to decrease the flow rate and temperatures were observed until the system again reached the adjusted steady-state.

The total heat transfer rate to the air flow is defined by the energy balance:

$$\dot{q} = \dot{m} c_p (T_{a,outlet} - T_{a,inlet}) \quad (1)$$

Here, $T_{a,outlet}$ and $T_{a,inlet}$ are the outlet and inlet air temperature, respectively, and c_p is the specific heat under constant pressure.

The bulk fluid temperature is defined as:

$$T_b = \left(T_{a,outlet} - T_{a,inlet}\right)/2 \quad (2)$$

Effective heat transfer coefficient is defined as:

$$h = \dot{q} / A_s (T_s - T_b) \quad (3)$$

where A_s is the total inner tube heated surface area and T_s is the mean of the surface temperatures measured by the type K thermocouples.

Reynolds number is defined as:

$$\mathrm{Re} = \frac{u\left(d_o - d_i\right)}{\nu} \quad (4)$$

where, d_o and d_i are the outer and inner diameter of the annulus, respectively. ν is the kinematic viscosity of the fluid and u is the mean Darcy velocity.

Nusselt number is defined as:

$$Nu = \frac{h\left(d_o - d_i\right)}{k} \quad (5)$$

k is the thermal conductivity.

Figure 4 shows test results for both copper and nickel foams. The results are plotted based on heat transfer coefficient versus pressure drop. Reynolds number was calculated using the hydraulic diameter of the annulus and the Darcy velocity. The highest Reynolds number exceeds 40,000. Both copper and nickel foams show similar heat transfer and pressure drop characteristics and magnitudes. The nickel foam data exhibit scatter due to physical characteristics peculiar to the nickel material (which is harder than copper), rougher ligament surfaces and edges.

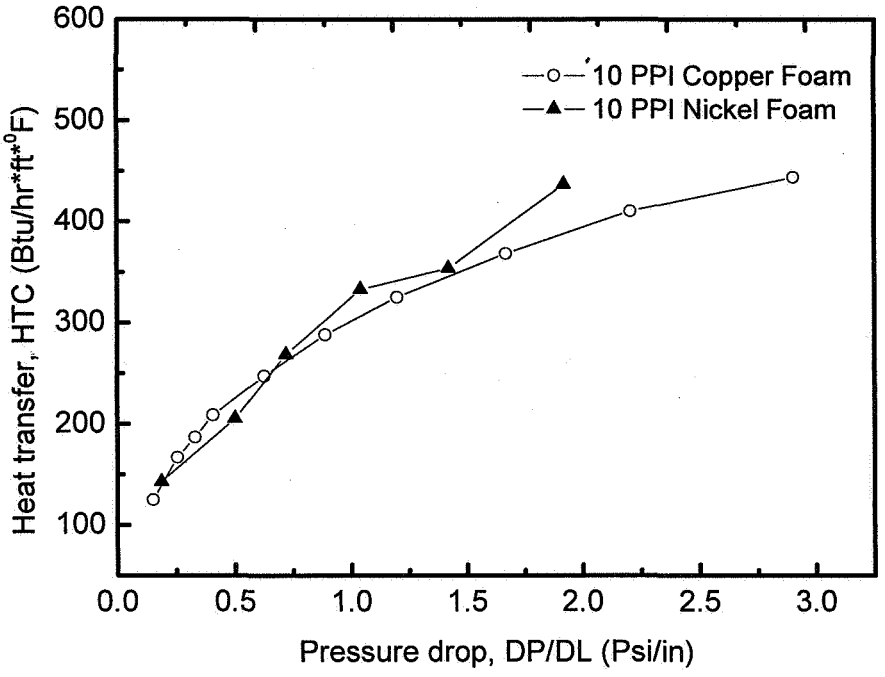

Figure 4: Experimental data

Experimental heat transfer data for 10 pore-per-inch copper and nickel foams were projected to performance of 20 and 40 pore-per-inch foams using the correlations of Leong and Jin [8] to illustrate trends in foam characteristics. These results are shown in Figure 5. Increasing the foam density also increases the pressure drop. Also included in Figure 5 is a correlation of heat transfer coefficient as a function of pressure drop for a microchannel heat exchanger as generated using a correlation of Indropera and DeWitt [10]. The important feature of this comparison is that for the laboratory conditions considerable heat transfer coefficient increases are obtained at the same pressure drop using open cell foam.

Comparisons between an open microchannel heat exchanger and foam-filled channels are contained in Tables 1 and 2. Table 1 compares foam-filled channel heat transfer coefficient with open channel heat transfer coefficient at an equal pressure drop. For instance, at 2 psi/in pressure drop, the heat transfer coefficient increases from 166 BTU/hr-ft-F to 451 BTU/hr-ft-F for a 40 ppi foam, an increase of 285 BTU/hr-ft-F or 172%. Similar increases are shown for the three foam sizes. Furthermore, the percentage enhancement is relatively independent of the pressure drop gradient. The enhancement is around 135%, 160% and 170% for 10 ppi, 20 ppi and 40 ppi, respectively.

Table 2 provides the required velocities in the two types of channels for the same pressure drop. Continuity requires that channel area increase as velocity decreases. The results indicate that the foam channel should be three times larger than the micro open channel in order to maintain the same mass flow rate. If both channels have the same

base width, the height of the foam filled channel therefore should be three times taller to maintain equal mass flow rates with the microchannel.

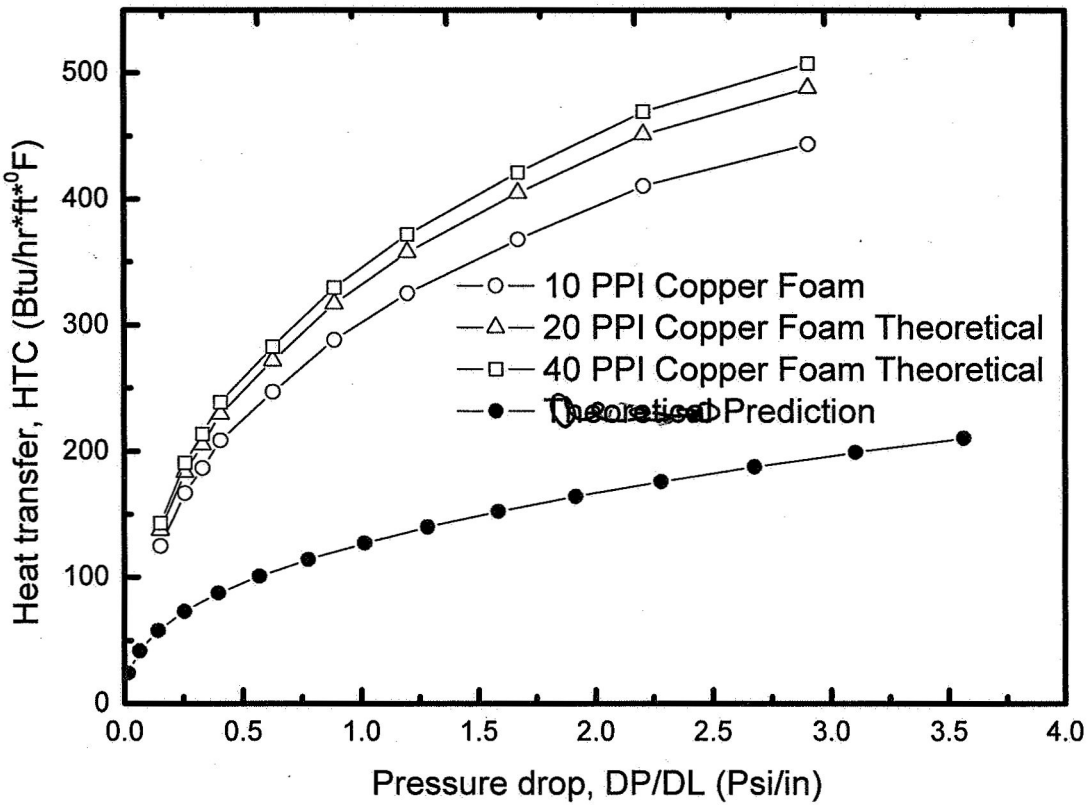

Figure 5: Comparison of Open Channel and Foam-Filled Channel Heat Transfer Coefficients.

Pressure Drop (Psi/In)	percent enhancement over microchannel for 10 PPI metal foam	percent enhancement over microchannel for 20 PPI metal foam	percent enhancement over microchannel for 40 PPI metal foam)
1.0	136%	160%	170%
1.5	137%	160%	171%
2.0	137%	161%	172%
2.5	131%	154%	165%
2.75	130%	153%	164%

Table 1: Comparison of heat transfer coefficient increase, open channel to foam-filled channel

Pressure Drop (Psi/in)	Velocity in copper foam ft/s	Velocity in microchannel ft/s	Velocity Ratio
3.0	90	275	1:3.05
2.5	83	255	1:3.07
2.0	77	225	1:2.92
1.5	68	197	1:2.89
1.0	58	160	1:2.76
0.5	43	116	1:2.7
0.15	20	63	1:3.15

Table 2. Velocity Ratio at Equal Pressure Drop

The above results from laboratory test with foam-filled cooling channels suggest an approach to evaluating channels at large Reynolds numbers, namely increasing the foam-filled channel cross-section to avoid increasing pressure drop. This strategy will be applied in future work, and a notional description of this approach is contained in the last section of this paper.

Numerical Simulations

Analytical CFD based models of a conventional microchannel heat exchanger and a foam filled heat exchanger were developed using FLUENT. These models enable calculation of heat transfer performance characteristics such as coolant temperature rise, pressure drop, total heat transferred, and heat transfer coefficients for comparison of the two types of heat exchangers at rocket conditions.

For comparison to the porous foam filled heat exchanger, a conventional microchannel heat exchanger model was created. A diagram of the open-channel model is shown in Figure 6. This physical channel and flow conditions were based on and derived from AIAA Paper 2005-4302, which summarizes on-going research at Purdue University. The channel has an internal cross-section of 2 mm x 4 mm. The other dimensions and operating parameters are listed in Table 3. Constant wall temperature of 1500 R is imposed as a boundary condition on the outer surface of the bottom channel wall to simulate effects of the combustion region. The top channel wall is insulated on the outside. The channel is unheated for the first 10 inches, the heated for the remaining 20 inches.

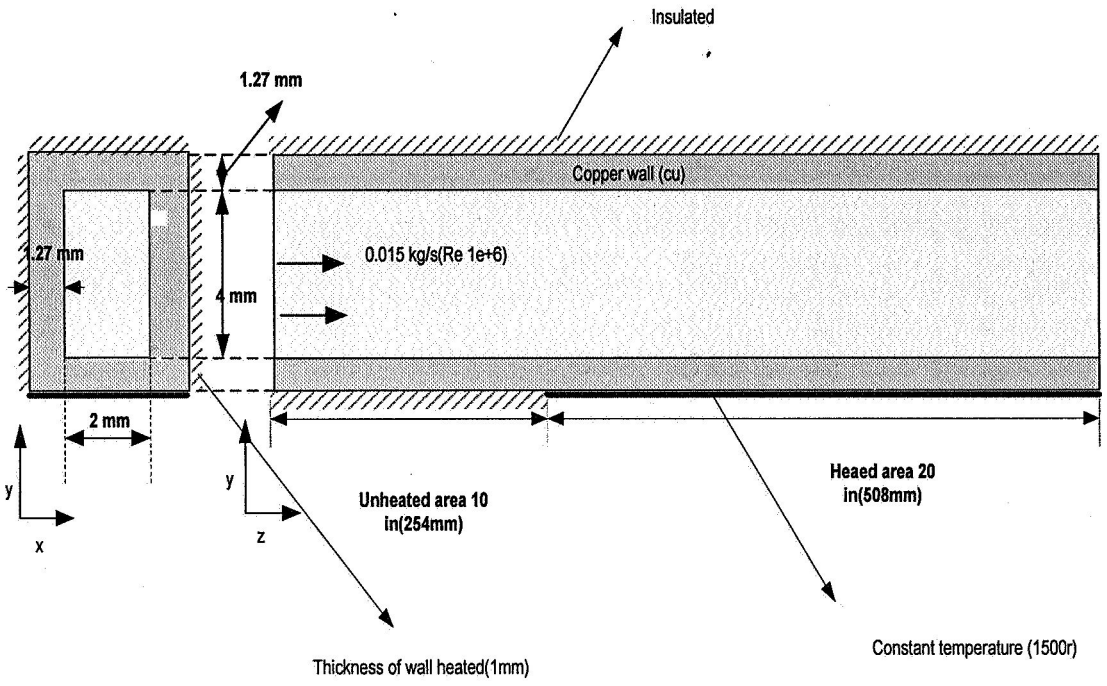

Figure 6: Schematic of the open channel Fluent model

Working fluid	Inlet Temperature	Outlet Pressure	Temperature of heated section	Mass flow rate (Re)	Length of unheated section	Length of heated section	Channel width	Channel height	Thickness of heated wall	Thickness of side and top walls
H2	200R	1000 psi	1500R	0.015kg/s (1x10**6)	10 in	20 in	.0787 in (2 mm)	0.157 in (4mm)	0.040 in (1mm)	0.05 in (1.27mm)

Table 3: Channel parameters

The conventional microchannel results are shown in figures 7-10. Figure 7 shows coolant (hydrogen) bulk temperature change over the channel length. Inlet-to outlet temperature increase of 540R was calculated. Figure 8 shows calculated coolant pressure drop, which was 317 psi. Temperature increase and pressure drop are largest in the heated section, with the unheated entrance section having smaller effects. Figure 9 shows cross section temperature distributions for two downstream locations, z=15 and 25 inches (5 and 15 inches into the heated section). Figure 10 is a diagram of total heat flux in the channel heated section. The total heat transfer rate of 63,190.83 watts is for the total bottom outer heated surface area, that is (2x1.27+2) mm x 508 mm = 2306.32 mm^2. Of the total heat transfer, 21.1% comes from the inner bottom surface, 62.6% from the side walls and only 15.3 percent from the top inner surface.

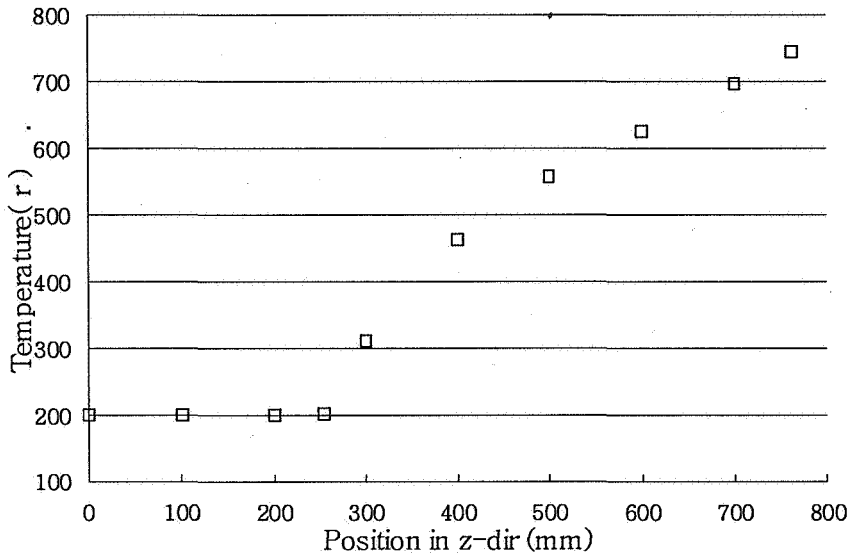

Figure 7: Coolant temperature increase

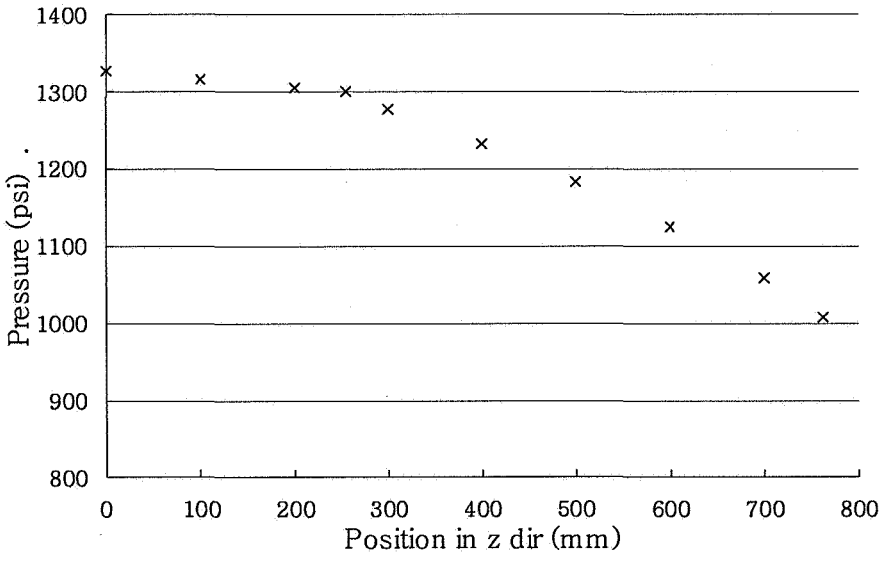

Figure 8: Coolant pressure drop

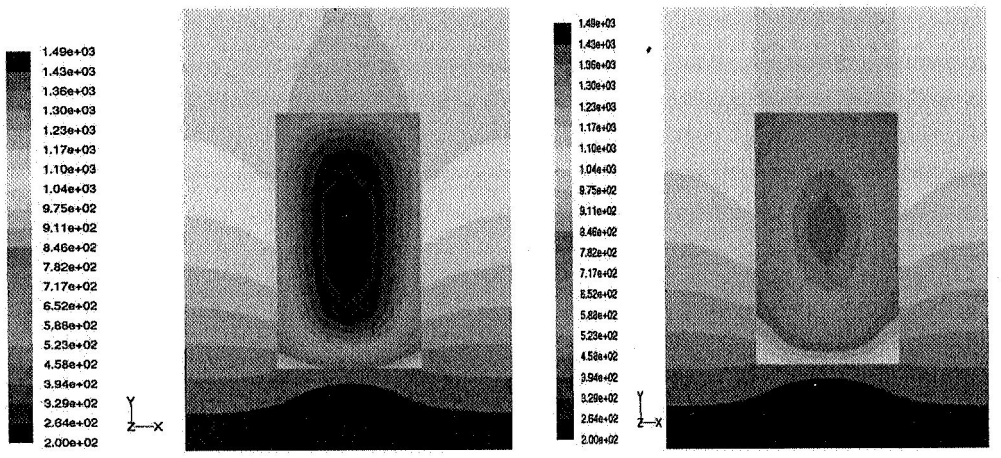

z=15 in z=25 in

Figure 9: Coolant and wall temperature cross-section distributions at z=15 and 25 in.

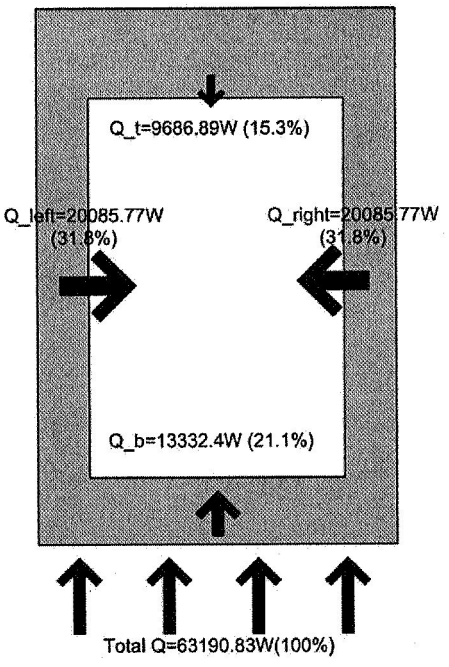

Figure 10: Heat transfer rates

A multi-ligament cell mesh has been developed to model the porous metal foam heat exchanger. The metal foams used in the experiments were produced using advanced material processing techniques that typically yield a microstructure of thin ligaments

(0.2-0.3 mm in diameter) forming a network of interconnected open-cells. Figure 11 is a photograph of the foam. The numerical model mimics the metal foam cells. The foam cell shape was based on Kelvin's tetrakaidecahedra. The geometry was created using the Solid Modeler Mechanical Desktop and has a porosity of approximately 0.977. The geometry was exported as an IGES file, and imported into the meshing software Gambit which is part of the FLUENT code. Figure 12 shows the 2-d and 3-d ligament networks developed for the numerical model. Fig. 13 shows the detailed mesh pattern used in the Fluent model. Different mesh sizes have been examined to determine a grid independent solution. The mesh has 1,138,016 nodes and is presented in Figures 13 and 14. Figure 13 shows the mesh configuration on the surface of the solid metal ligaments. Figure 14 provides the mesh structures of the surfaces that are located at the periodic and wall boundaries. Additionally, the results to date have been run with air as an ideal gas and the kω-SST turbulence model.

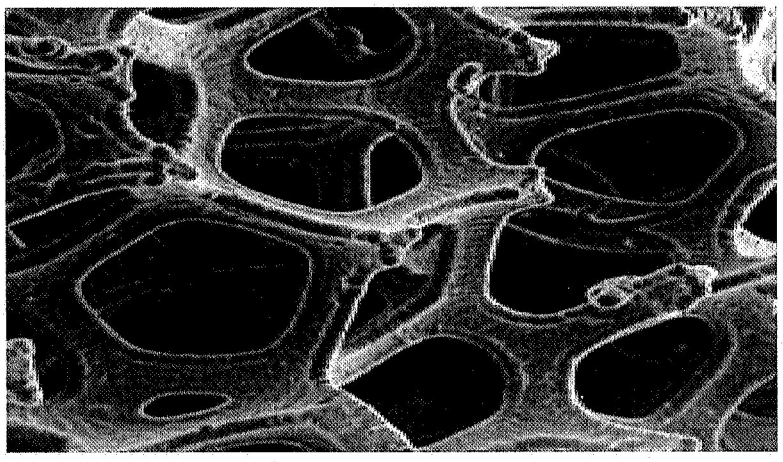

Figure 11: Photograph of open cell foam

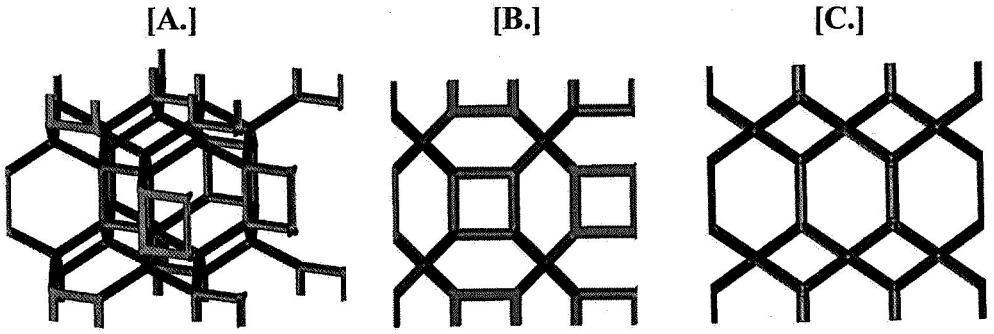

Figure 12. [A] Iso-Metric View of Model Foam [B] View Looking with the Flow (Flow Direction is into the page) [C] View Looking Perpendicular to the Flow (Flow is from left to right)

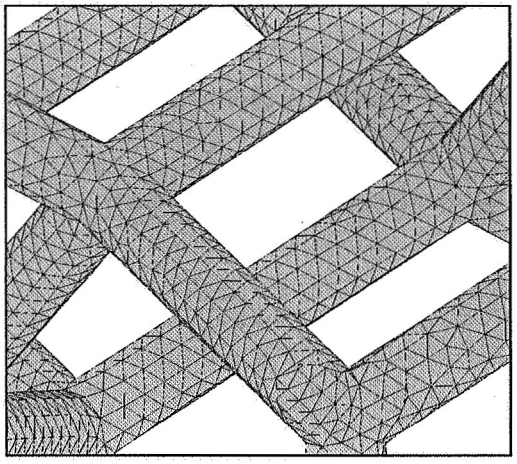

Figure 13: Computational mesh on the surface of the metal ligaments

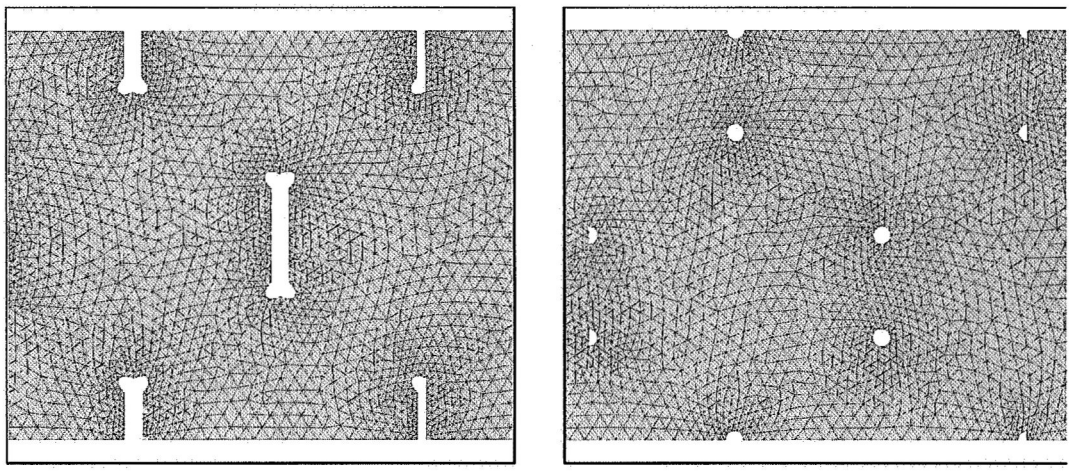

Periodic surface wall surface

Figure 14: Computational mesh configurations on the periodic and wall boundary surfaces.

Because of the unit cell structure of the metal foam and the highly demanding computational time requirement, a strategy has been developed to focus on two typical cells as illustrated in Figure 15.

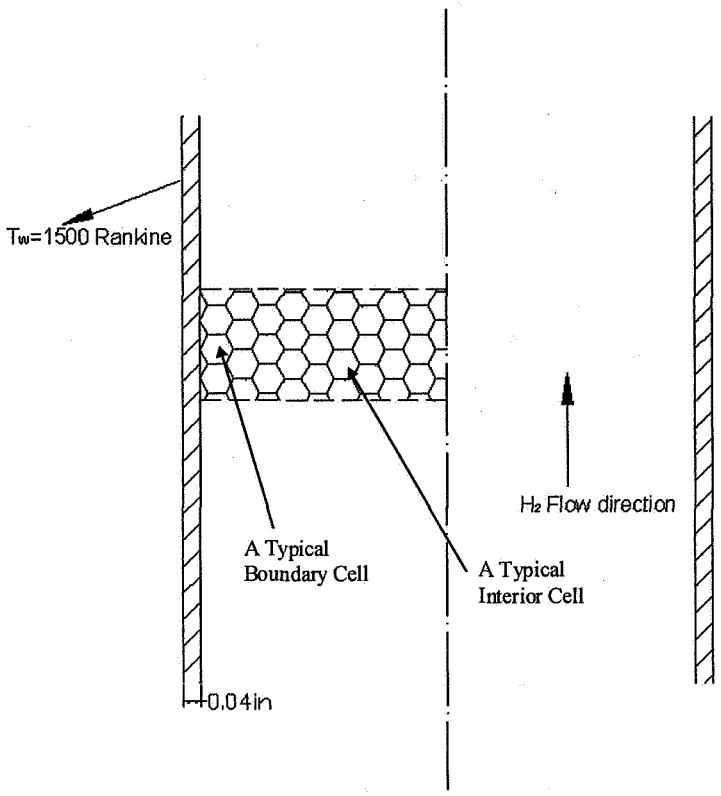

Figure 15: Typical cells

As a result, two computational models have been created. The first represents a typical interior cell and is termed the "periodic" model because periodic or symmetric boundary conditions are applied in all directions except in the stream-wise direction. A diagram of this is shown in Figure 16.

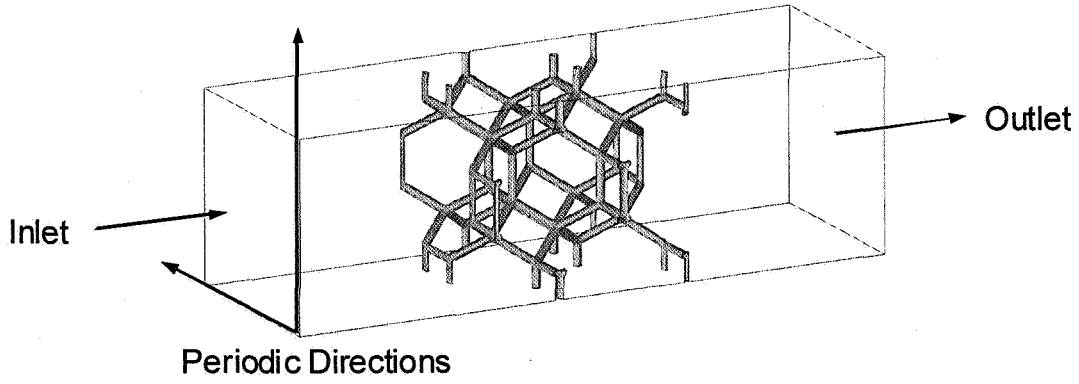

Figure 16. Periodic Model

The second model treats the cell that is attached to the wall and is termed the "wall / symmetry" model. Here, periodicity is applied in only one direction. In the other

direction one boundary was set as a wall and the remaining boundary as a symmetry plane. This is shown in Figure 17.

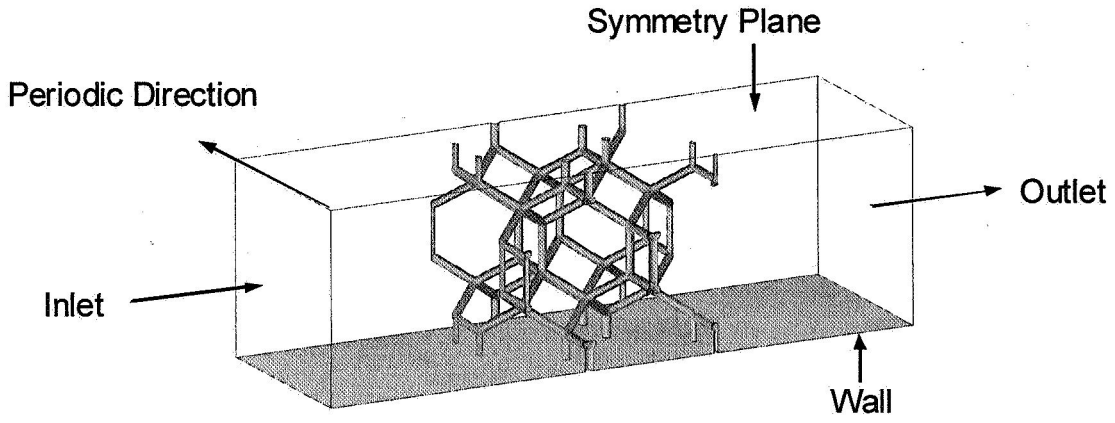

Figure 17: Wall / Symmetry Model

Open cell foam computational models are now being used to produce analytical results. Figures 18 and 19 show qualitative features of flow through open cell foam, gage pressure contours and velocity contours on the periodic boundaries. Flow is left to right.

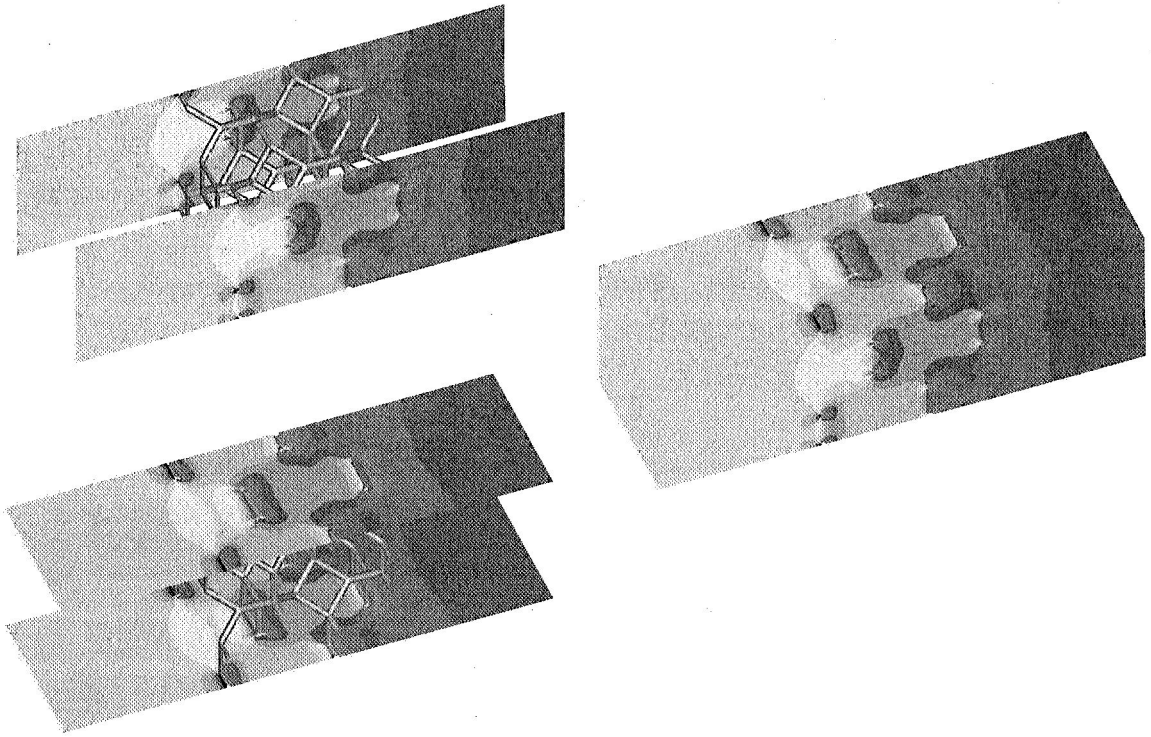

Figure 18: Static Pressure (Gauge) Contours on the Periodic Boundaries (Red is High, Blue is Low).

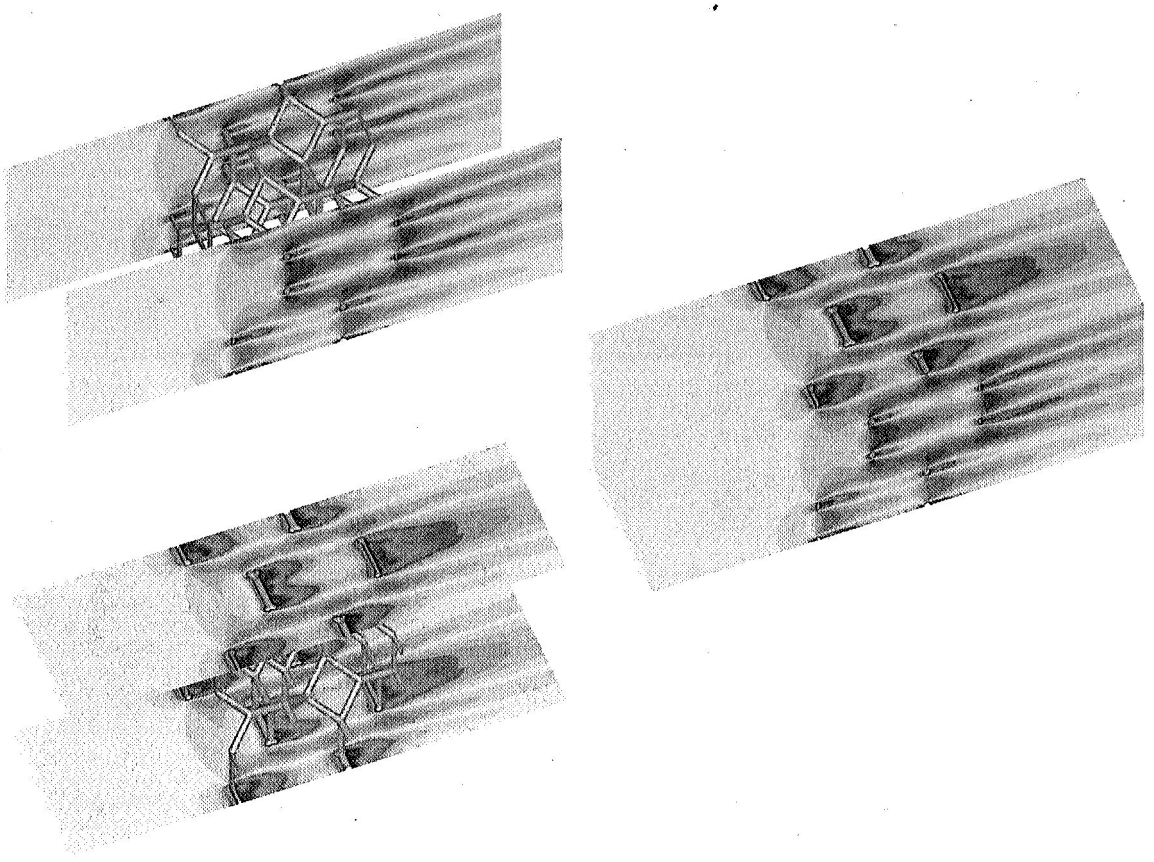

Figure 19: Velocity Magnitude Contours on the Periodic Boundaries (Red is High, Blue is Low)

Wakes from cell ligaments and high velocities in between ligaments are evident in figure 19.

Experimental data from Leong and Jin [8] have been chosen to assess the fidelity of our model. Figure 20 shows the comparison between the numerical results and experimental results from [8] for the 10 ppi case. As seen from Fig. 20, both the periodic model and wall/symmetric model under-predict slightly the experimental results. The trends of the experimental data and those of the current numerical simulation are identical and therefore, the deviations between the two are of a fixed percentage value. This type of errors is called the fixed error or precision error. One source of deviations is that the actual metal foams have rough edges while the numerical model is based on smooth thin cylinders. Another factor is that visual observation of the test foam showed that a small number of pores are actually totally sealed which will contribute to the higher pressure drops. Considering these factors and that the experimental uncertainties were ±30%, the numerical simulations are judged acceptable.

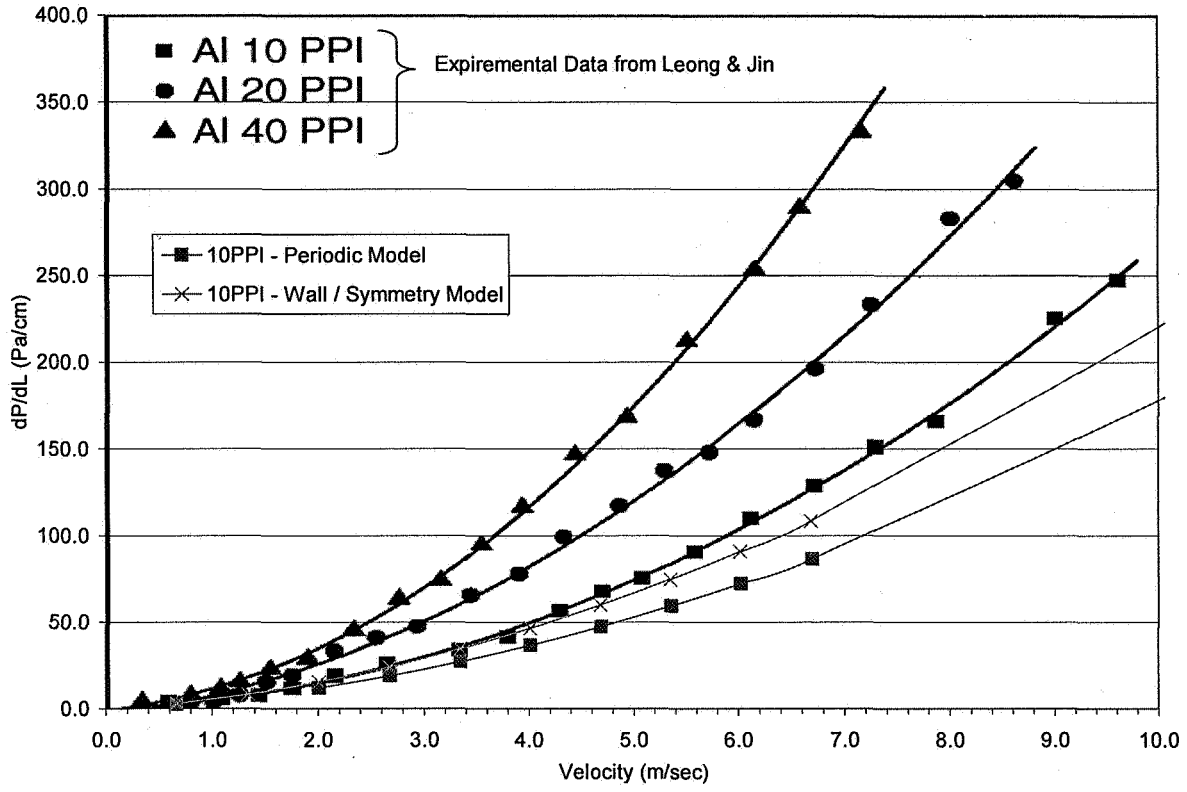

Figure 20. Pressure Drop vs. Average Velocity and Compared to the Results of Leong and Jin [8]

Finally, the models have been employed to predict the pressure drop per unit length for 5, 10 and 20 ppi foams at a number of different flow rates to develop a set of pressure drop curves. Figure 21 shows the pressure drop gradient verse velocity for a range of cell sizes. All the curves have similar trends which indicate a laminar flow regime for the velocity less than around 10 m/s and than a transition to turbulent flows. In general, the pressure drop gradient increases with decreasing pore sizes. The pressure drop gradient for the 10 ppi is about 150% higher than that of the 5 ppi and the 20 ppi pressure drop gradient is also about 150% higher that the 10 ppi. For both 5 ppi and 10 ppi, the pressure drop gradient for the wall model is about 15% higher than the interior model. It is noted that the top curve in Fig. 21 is the pressure drop gradient for hydrogen coolant in a 10 ppi metal foam as a function of velocity. The thermodynamic properties for the hydrogen were based on the pressure and temperature levels calculated in the microchannel for rocket conditions given in Figures 7 and 8. The hydrogen pressure drop gradient is 2.7 times higher than that of air in a 20 ppi metal foam under the same velocity.

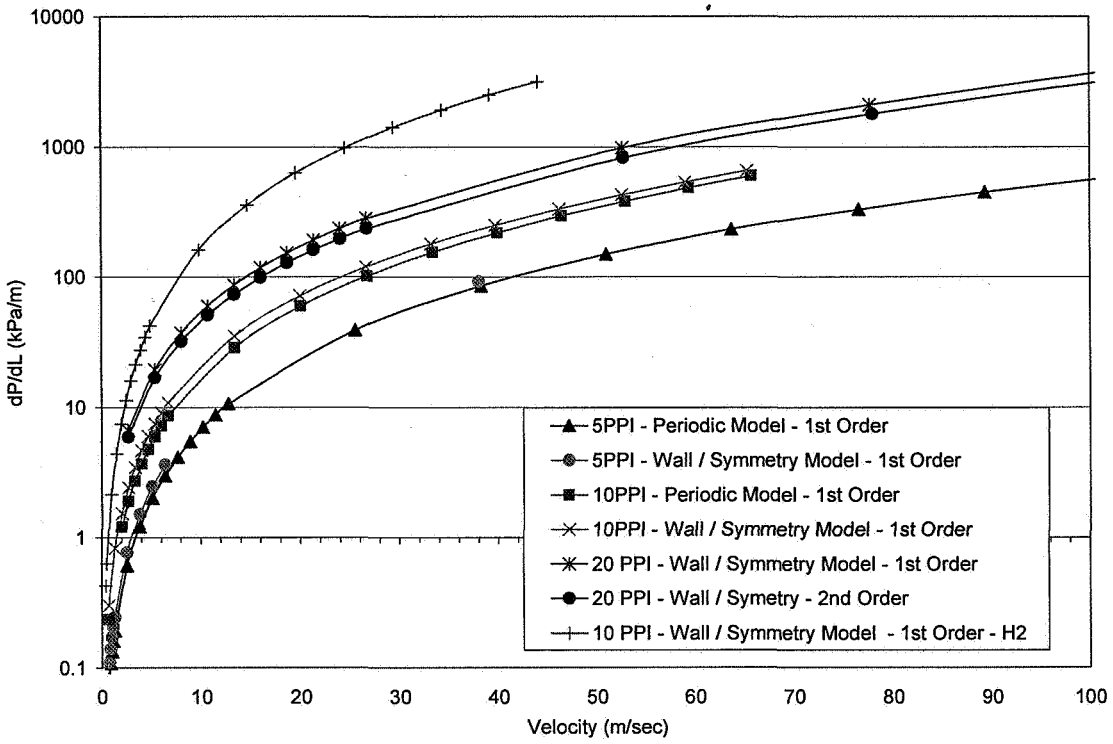

Figure 21. Pressure Drop vs. Mass Flow Rate

Status and Work Remaining

As described above, laboratory tests comparing open cell foam-filled cooling channels with conventional, unfilled open cooling channels demonstrated large heat transfer enhancements. Experiments performed extended the Reynolds number range relative to data found in the literature. Analytical heat transfer models of open-cell foam filled channels have been created to extend the Reynolds number range, and initial applications of the models are underway. The numerical models will be used to evaluate cooling circuit characteristics at high Reynolds number rocket chamber conditions.

The models will be used to calculate coolant heat pickup and pressure drop as well as wall temperature profiles, and relevant quantities such as heat transfer coefficients will be derived. Detailed comparisons of parameters for open channel and foam-filled channels will be made.

The design strategy suggested in the laboratory experiment section will be used to design foam-filled channels and heat transfer comparisons with open channels will be made. Specifically, channel cross section area will be increased and velocity in the foam-filled channel will be decreased to avoid increasing pressure drop, and heat transfer changes relative to an open channel will be calculated. Comparisons with open channels will be made at an equal pressure drop. This strategy is shown schematically in figure 22. As suggested in Tables 1 and 2, it is anticipated that reasonable increases (~3x) in channel cross section will result, followed by heat exchanger designs that are not large departures from those found in existing rocket chambers.

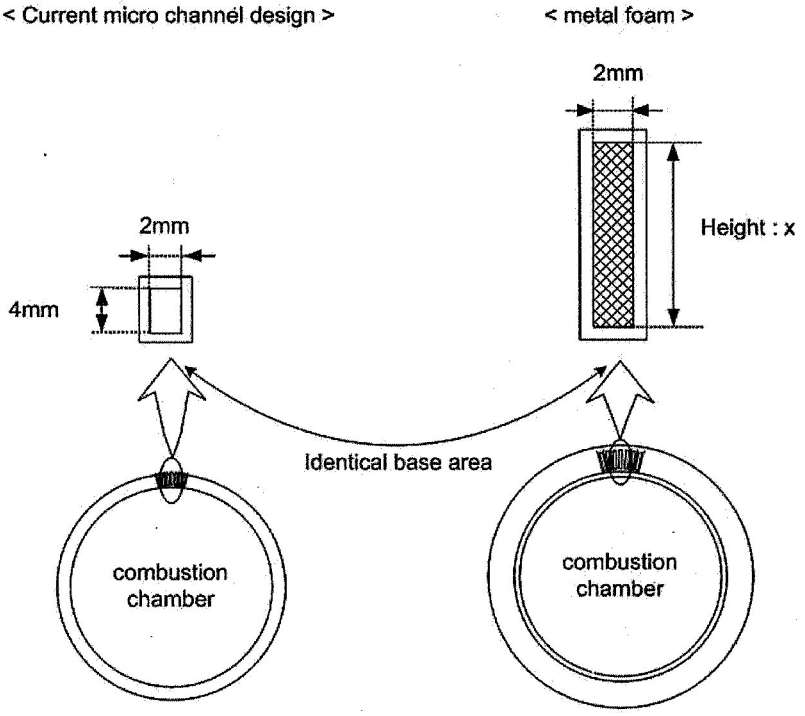

Figure 22. Notional design strategy for foam-filled channels

Acknowledgment

This work has been performed with support from NASA grant NCC3-994 (Constellation University Institute Program) with Claudia Meyer as the Program Manager.

References

[1] Koh, J.C.Y. and Colony, R., 1974, Analysis of Cooling Effectiveness for Porous Material; in a Coolant Passage, *J. Heat Transfer*, **96**, 324-330.

[2] Koh, J.C.Y. and Stevens, R.L., 1975, Enhancement of Cooling Effectiveness by Porous Materials in Coolant Passage, *J. Heat Transfer*, **97**, 309-311.

[3] Maiorov, V.A, Polyaev, V.M., Vasilev, L.L. and Kiselev, A.I., 1985, Intensification of Convective Heat Exchange in Channels with a Porous High-Thermal-Conductivity Filler. Heat Exchange with Local Thermal Equilibrium Insude the Permeable Matrix, *J. Engineering Physics*, **47**, 748-757.

[4] Hunt, M.L. and Tien, C.L., 1988, Effects of Thermal Dispersion on Forced Convection Fibrous Media, *Int. J. Heat Mass Transfer*, **31**, 301-309.

[5] Bartlett, R.F. and Viskanta, R., 1996, Enhancement of Forced Convection in an Asymmetrically Heated Duct Filled with High Thermal Conductivity Porous Media *J. Enhanced Heat Transfer*, **6**, 1-9.

[6] Kuzay, T.M., Collins and Koons, J., 1999, Boiling Liquid Nitrogen Heat Transfer in Channels with Porous Copper Inserts, *Int. J. Heat mass Transfer*, **42**, 1189-1204.

[7] Boomsma, K., Poulikakos, D. and Zwick, F., 2003, Metal Foams as Compact High Performance Heat Exchangers, *Mechanics of Materials*, **35**, 1161-1176.

[8] Leong, K.C. and Jin, L.W., 2006, Effectof Oscillatory Frequency on Heat Transfer in Metal Foam Heat Sink of Various Pore Densities, *Int. J. Heat mass Transfer*, **49**, 671-681.

[9] Lu, W., Zhao, C.Y. and Tassou, S.A., 2006, Thermal analysis on Metal-Foam Filled Heat Exchangers Part I : Metal-Foam Filled pipes, *Int. J. Heat mass Transfer*, **49**, 986-997.

[10] Incropera, F. and DeWitt, D., 2003, Fundamentals of Heat and Mass Transfer, Wiley, New York, N.Y.

[11] Wennerberg, J.C, Anderson, W.E., Haberlen, P.A., Jung, H. and Merkle, C.L., "Supercritical Flows in High Aspect Ratio Cooling Channels", AIAA Paper 2005-4302, 41st AIAA/ASME/SAE/ASEE Joint Propulsion Conference and Exhibit, Tucson, Arizona, July, 2005.